Atlantic bluefin tuna (*Thunnus thynnus*): a state-dependent energy allocation model for growth, maturation, and reproductive investment

Erik W. Chapman, Christian Jørgensen, and Molly E. Lutcavage

Abstract: The relationship between Atlantic bluefin tuna (ABFT, *Thunnus thynnus*) life history patterns and environmental conditions was investigated by developing a state-dependent model that optimizes energy allocation between growth and energy stores and the decision to spawn. The model successfully recreates growth, age-at-maturity, and seasonal variability in condition for western ABFT that spawn primarily in the Gulf of Mexico. Eastern ABFT spawning in the Mediterranean Sea display a life history trajectory shifted toward earlier maturation and, perhaps, reduced growth — a pattern predicted by the model when mortality was higher, migration distance shorter, and food intake during migration and spawning higher. Simulations highlight the sensitivity of the optimal ABFT life history strategy to variability in net energy intake, particularly during migration and spawning, a poorly understood component of their life cycle. Results also emphasize the importance for optimal life history patterns of the timing of spawning migrations in relation to the phenology and amplitude of seasonal prey availability. This study provides insight into potential mechanisms that underlie observations that are at the heart of current discussions regarding ABFT subpopulation structure and variable life history patterns.

Résumé : La mise au point d'un modèle dépendant de l'état qui optimise l'allocation d'énergie entre la croissance et les réserves énergétiques et la décision de frayer a permis d'étudier la relation entre les patrons du cycle biologique du thon rouge (ABFT, *Thunnus thynnus*) et les conditions de l'environnement. Le modèle représente avec succès la croissance, l'âge à la maturité et la variabilité saisonnière de la condition chez les ABFT de l'ouest qui fraient principalement dans le golfe du Mexique. Les ABFT de l'est qui fraient dans la Méditerranée présentent une trajectoire de cycle biologique avec un déplacement vers une maturation plus hâtive et, peut-être, une croissance réduite — c'est un patron prédit par le modèle quand la mortalité est plus élevée, la distance de migration plus courte et l'ingestion de nourriture durant la migration et la fraie plus grande. Les simulations soulignent la sensibilité de la stratégie optimale du cycle biologique des ABFT à la variabilité de l'ingestion nette d'énergie, particulièrement durant la migration et la fraie, une composante mal comprise de leur cycle biologique. Les résultats soulignent aussi l'importance pour l'obtention de patrons optimaux du cycle biologique d'un calendrier des migrations de fraie en relation avec la phénologie et l'amplitude de la disponibilité saisonnière des proies. Notre étude ouvre une perspective sur les mécanismes potentiels qui sous-tendent les observations qui alimentent les discussions actuelles sur la structure des sous-populations et les patrons variables du cycle biologique des ABFT.

[Traduit par la Rédaction]

Introduction

In speed, grace, and hunting effectiveness, tuna are virtually unmatched among marine top predators. The elusive, nomadic lifestyle of tuna species makes them a challenge for scientists, managers, and fishermen — a fact that may be responsible for the continued persistence of this species despite centuries of exploitation. However, in recent decades Atlantic bluefin tuna (ABFT, *Thunnus thynnus*), a commercially valuable migratory tuna with a basin-scale distribution, have become the focus of increasing fishing pressure (ICCAT 2009), raising questions concerning the fish's sustainability under current management practices (ICCAT 2009; Fish and Wildlife Service 2009). The International Commission for the Conservation of Atlantic Tunas (ICCAT) is responsible for managing ABFT, which it delineates as a western (W-BFT) and an eastern (E-BFT) stock. ICCAT's two-stock management approach is supported by differences in life history characteristics (E-BFT mature smaller and earlier than W-BFT), and there appears to be regional natal homing to the spawning grounds in the Mediterranean Sea and Gulf of Mexico, respectively (Secor 2002; Rooker et al. 2008).

Received 3 January 2011. Accepted 5 July 2011. Published at www.nrcresearchpress.com/cjfas on xx November 2011.
J2011-0005

Paper handled by Associate Editor Ray Hilborn.

E.W. Chapman. New Hampshire Sea Grant, University of New Hampshire Cooperative Extension, 131 Main Street, Durham, NH 03824, USA.
C. Jørgensen. Uni Research, Bergen, Norway.
M.E. Lutcavage. Large Pelagics Research Center, Department of Conservation Biology, University of Massachusetts Amherst, Gloucester, MA 09130, USA.

Corresponding author: Erik W. Chapman (e-mail: erik.chapman@unh.edu).

Life history trajectories can reflect the environment a fish population experiences and has adapted to, though the reasons for observed differences in life history between the stocks are not understood. For example, E-BFT migration distance appears to be shorter (although this assumption deserves further study), and these fish have experienced more intense fishing pressure for a longer time than W-BFT (Fromentin and Powers 2005).

Overall, a great deal of uncertainty remains regarding basic life history traits and population substructure for this species, particularly for W-BFT (Fromentin and Powers 2005; Rooker et al. 2007; Galuardi et al. 2010). For example, the presence of presumably mature fish outside the known spawning areas during the breeding period (Lutcavage et al. 1999; Block et al. 2005; Galuardi et al. 2010) suggests that either unknown spawning areas are available to ABFT or skipped spawning is a common behavior for this species. Some of this uncertain information forms the basis of calculations of ABFT stock productivity forecasts, rebuilding potential, and threshold fishing mortality that are key components of the current ICCAT management approach (ICCAT 2007; Secor 2007). Addressing these uncertainties and improving our understanding of the interplay between life history traits and population structure is important for improving the effectiveness of ABFT management (Rooker et al. 2007; ICCAT 2009).

Life history models can be useful tools for exploring the theoretical interplay among ecosystem conditions and emerging life history traits, spawning behavior, and seasonal variability in condition resulting from allocation strategies for fish species (Jørgensen and Fiksen 2006; Jørgensen et al. 2006, 2008). Our primary objective is to develop such a model that recreates observed patterns in population characteristics (growth, age-at-maturity, seasonal changes in condition) for ABFT. By exploring the interplay between environmental conditions and ABFT population characteristics, we obtain insight into potential mechanisms responsible for observed differences between E-BFT and W-BFT and examine whether skipped spawning would be an optimal spawning behavior for this species.

To meet these objectives, we developed a state-dependent model of growth, maturity, and energy allocation to reproduction. In this model, ABFT growth, condition (length–mass relationship), age-at-maturity, and size-at-age relationships emerge from the interaction among environmental conditions and the individual energy allocation and spawning strategy that is optimal in that environment. Simulations were selected to explore the influence of key environmental variables that may differ between ABFT subpopulations, which include distance between feeding and spawning areas, food ingestion during migration and spawning, and an annual mortality rate that integrates natural and fishing mortality.

We have included functional relationships from theory or other species where ABFT biology is scarce. For example, hydrodynamic costs of swimming have not been quantified for tuna of different condition factors, but hydrodynamics predicts that drag increases with cross-sectional area (Vogel 1994). We've implemented increasing swimming costs with increasing condition. With spawning costs, there is a fundamental difference between the energetic costs of getting to and from the spawning grounds and the timing of the migration, which can imply opportunity costs (or benefits). For example, foraging opportunities can be lost if an individual must leave the feeding area to migrate when feeding conditions are still good. Alternatively, foraging opportunities can be gained when individuals leave suboptimal feeding areas for better ones. Consequently, timing of migration incurs an added benefit or cost, as it determines the location of individuals in relation to seasonal food availability throughout a species' range (e.g., Varpe et al. 2007). Compare this with swimming costs, which are often less for smaller fish, thus involving energy units rather than time, and where functions and trade-offs are more likely to be linked to size. In our approach, we've modeled the costs of migration that includes both the costs and benefits associated with the timing and energetic costs of migration. A model for the purposes of this study that would include more specific processes (e.g., vertical migration behavior and thermoregulation) is not possible given the complex life history and current biological understanding of ABFT.

Our methodological direction aligns with mechanistically rich modeling (DeAngelis and Mooij 2003) and combines species-specific relationships, when known, with general relationships. This approach can reveal where our knowledge is sound, where critical gaps exist, and which parameters are most important to model behavior.

Materials and methods

Model overview

At monthly time steps, ABFT (*i*) feed, (*ii*) optimally allocate surplus energy to growth or to storage, and (*iii*) when optimal, either migrate to and from a spawning site where they use their stored energy to develop gonads or remain in the feeding area and continue to allocate energy to growth or storage. In addition to energy allocation and the decision to migrate and spawn, the level of stores that remain after spawning is also optimized. This cycle is repeated up to an effective maximum lifespan of 25 years. In reality, fish may live beyond 25 years, but the maximum age in the model represents an effective maximum age in terms of population-level reproductive effort. The optimization criterion is expected lifetime energy available for egg production, and the model only considers females. Energy allocation is state-dependent, with states being age (in months), body length (in cm), stored energy (proportion of full), and current level of food availability (needed because of the autocorrelated feeding environment).

Energy balance is calculated in different ways during time spent on the feeding area, during migration, and during spawning. ABFT make extensive vertical migrations each day to different environmental regimes (Lutcavage et al. 1999; Block et al. 2001; Wilson et al. 2005), presumably to maximize access to prey and to minimize stresses imposed by vertical distributions of temperature, oxygen, and predators. An additional important consideration is that large ABFT are warm-bodied (e.g., Carey and Lawson 1973; Lawson et al. 2010) and thus unique in comparison with most other pelagic fishes. In terms of their thermal and cardiorespiratory physiology, large size, heat retention systems, and other biochemical attributes confer distinct (but of course limited) advantages and allow ABFT to surpass thermal constraints encountered by most fishes, even of similar sizes.

Their body temperatures in the cool feeding grounds are actually 10–15 °C higher than ambient (Lawson et al. 2010). In this respect they're functional homeotherms, and while temperature and oxygen are certainly important factors determining ABFT behavior, it is assumed that these processes are most important at a smaller spatio-temporal scale than is the focus here.

For these reasons, during time spent in the feeding area (prior to maturity and otherwise when not either migrating or spawning), energy balance is assumed to reflect a seasonally varying and stochastic food environment. The modeled food environment during this time has both seasonality and autocorrelated stochasticity to reflect typical temporal patterns in prey availability and thus tuna foraging efficiency. During migration, energy balance reflects the energetic cost of movement (a function of the physical costs of movement and time spent away from potentially more productive feeding areas) and is modified by opportunistic feeding. During spawning, energy balance is a function of an estimated activity cost of spawning and again is modified by some opportunistic feeding.

The growth environment experienced by individual cohorts in the model varies according to the stochasticity imposed on the food environment of the feeding area. Thus, model results averaged over a long time period (thousands of years) allow several population characteristics and their variability to emerge, including growth trajectories, maturation ages and sizes, reproductive investment strategies, and population dynamics, including age and size structure.

The model used in this study is based on a similar approach for the Atlantic cod (*Gadus morhua*; Jørgensen and Fiksen 2006). The bioenergetics framework is built on the Wisconsin bioenergetics model (Hewett and Johnson 1992) but modified to fit parameters and relationships available for ABFT. Alternative frameworks for bioenergetics modeling include dynamic energy budgets (DEB; Kooijman 2000) and the metabolic theory of ecology (MTE, Brown et al. 2004). MTE is designed to be general and does not easily allow incorporation of species-specific parameters or relationships, but the reliance on allometric scaling resembles our approach. DEB allows easier incorporation of species detail, but contains assumptions that constrain the type of output a model can produce. For example, DEB assumes that allocation to reproduction happens over the entire lifetime, which might be appropriate for some organisms but less so for long-lived fish. In contrast, our approach is designed to study evolution of maturation and reproduction as flexible traits that emerge from evolutionary considerations. Fitness maximization combines a backwards iterating algorithm that produces an optimized life history plan (Houston and McNamara 1999; Clark and Mangel 2000) and a forward simulation that allows visualization of individual and population characteristics emerging from the interaction between the life history plan and environment. The proposed model is intended to be a generalized model that is not specified for either W-BFT or E-BFT, though the reference scenario is designed to represent conditions experienced by W-BFT.

Individual physiology

The individual body mass is compartmentalized into irreversible, structural mass and reversible, energy storage (Roff 1983). Structural mass ($W_{\text{Structure}}$, g) is a function of length and is calculated as

$$(1) \qquad W_{\text{Structure}}(L) = \frac{K_{\text{Min}} \cdot L^3}{100}$$

where K_{Min} is the minimum Fulton's condition factor (unitless) and L is the fish body length (cm), which we define as the straight fork length (cm).

wAdditional energy (E_{Stores}, kJ) above $W_{\text{Structure}}$ can be stored to meet energy demands of activity (migration, searching for prey), spawning (egg production, in the case of females), and starvation in periods of low food availability. ABFT primarily store energy as intramuscular lipid stores and proteins embedded in muscles, and prior to spawning additional lipids are stored as perigonadal fat. Here, energy stores are defined as the combined intramuscular and perigonadal fat stores and increased protein stored in the muscles. The mass in energy stores (W_{Stores}, g) is calculated as

$$(2) \qquad W_{\text{Stores}}(E_{\text{Stores}}) = \frac{E_{\text{Stores}}}{\rho_{\text{Stores}}}$$

where ρ_{Stores} (kJ·g^{-1}) is the wet-mass energy density of stores.

The total mass of the tuna ($W_{\text{Total}}(L, E_{\text{Stores}})$, g) can then be calculated as

$$(3) \qquad W_{\text{Total}}(L, E_{\text{Stores}}) = W_{\text{Structure}}(L) + W_{\text{Stores}}(E_{\text{Stores}})$$

A second parameter, K_{Max}, sets the maximum amount of energy stores that can be carried by an individual fish ($E_{\text{MaxStores}}$, kJ):

$$(4) \qquad E_{\text{MaxStores}}(L) = \rho_{\text{Stores}}(K_{\text{Max}} - K_{\text{Min}})\frac{L^3}{100}$$

The values for K_{Min} and K_{Max} were estimated based on an analysis of length and mass data for 4830 ABFT between 185 and 305 cm (8- to 25+-year-old fish; Turner and Restrepo 1994) from commercial fishery landings in the Gulf of Maine region. These data were collected across the period when ABFT condition is expected to be at a minimum (June, following spawning) and at a maximum (November, at departure from primary feeding area). The values for K_{Min} and K_{Max} were set at two standard deviations from the mean Fulton's K value for the length and mass data set.

Energy budget overview

A net intake function for a fish carrying no energy stores, modified by seasonal and stochastic variability in the food environment, is used to calculate the amount of energy ingested by an individual fish. The intake function is further modified by subtracting the cost of carrying energy stores (lipids), which is a metabolic cost assumed to be less than that for carrying somatic tissue. If a positive amount of energy remains after the cost of carrying stores is subtracted from the intake function, energy is ingested and a variable proportion of energy is allocated toward either growth (increasing length and structural mass) or energy stores (increasing mass of stored lipids and proteins). If a negative energy value remains, the energy deficit is drawn from energy stores.

Energy intake

A single function for net energy intake is used. Net energy intake is the difference between ingested energy available for production and all metabolic costs. As such, the net intake function integrates variability in prey availability, prey quality, and metabolic costs over time and accounts for digestive inefficiency. This approach minimizes the potential for compounding uncertainties associated with an estimation of each of the integrated processes.

The average net energy intake (I, kJ·month^{-1}) of a lean tuna is assumed to be an allometric function of fish length:

$$(5) \qquad I(L) = a \cdot L^b$$

The coefficient a (kJ·cm^{-b}·month^{-1}) is set to match observed growth for the species, and the exponent b (unitless) is derived from published estimates for the scaling of ingestion and metabolic costs with ABFT mass (Overholtz 2006; Fitzgibbon et al. 2008).

To introduce individual variability in the model, the average intake I is modified by two components of environmental variability (seasonality and temporally autocorrelated stochasticity) and one component of individual variability (the metabolic cost of the individual's stores, C_{Stores}):

$$(6) \qquad I_{\text{Net}}(L, E_{\text{Stores}}, t) = I(L) \cdot [S(t) + X(t)] - C_{\text{Stores}}(E_{\text{Stores}})$$

Here $S(t)$ is seasonal variability in prey availability and quality, and stochasticity $X(t)$ represents the inherent background variability in the food environment.

Seasonality

The majority of annual growth in length for juvenile ABFT occurs between June and November in both the eastern and western Atlantic (Mather and Shuck 1960; Furnestin and Dardignac 1961; Cort 1991). This suggests that ABFT experience strong seasonality in net intake as a consequence of annual cycles in environmental components that influence the difference between energetic intake and metabolic costs. Presumably, the seasonality in net intake reflects variability in photoperiod, prey aggregation, and prey quality in their primary feeding areas. These processes are integrated in a seasonality term that is set initially as a sine function of day-of-year ($S(d)$) that is characterized by an amplitude (S_{Amp}, unitless) and mean (S_{Mean}, unitless) value and a day that the seasonal peak intake occurs (D_{Peak}, day of year) (Fig. 1*a*):

$$(7) \qquad S(d) = S_{\text{Mean}} + \sin\left[\frac{d + \pi(90 - D_{\text{Peak}})}{360}\right] \cdot S_{\text{Amp}}$$

A sine function was selected because seasonality is expected to approximate seasonal variability in photoperiod, which approximates a sine curve over an annual cycle. Monthly mean values are calculated from the daily seasonality function as required by the monthly model time step. Calculating seasonality on a daily time scale allows for peak seasonality to be varied by time increments of less than a month. The initial setting for the seasonal peak is set as 15 August based on an estimated time when ABFT are gaining mass at the greatest rate in higher-latitude feeding areas (W. Golet and M. Lutcavage, unpublished data; Mather and Shuck 1960).

Fig. 1. Variability in the value for annual seasonality (*a*) and a 25-year example of variability in environmental stochasticity (*b*) and the environment conditions (combined seasonality and environmental stochasticity) (*c*) that determine net energy intake in the feeding area.

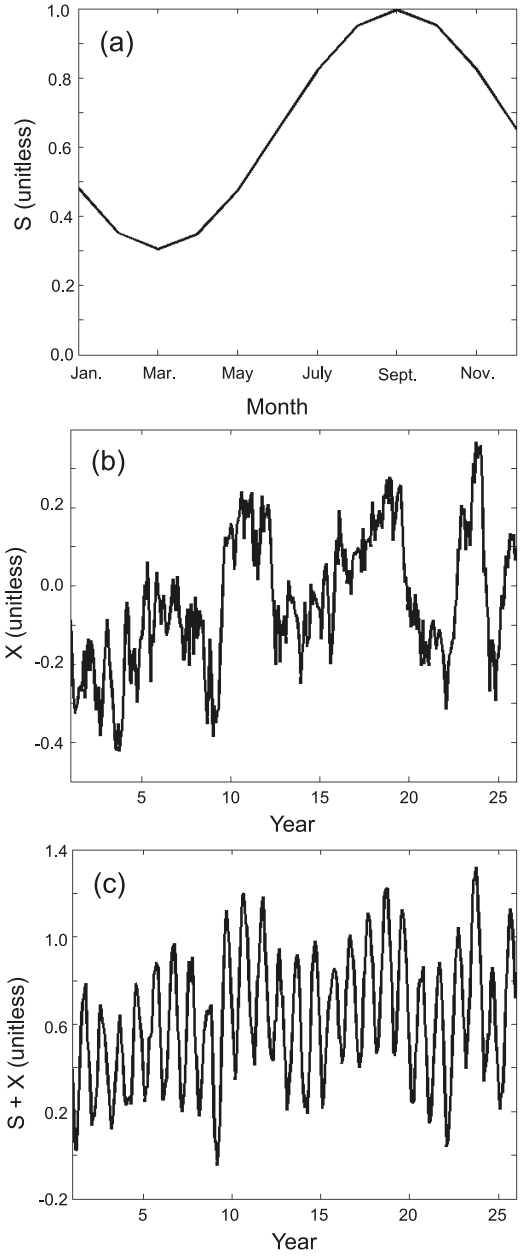

Stochasticity

Food intake in the model is also modified by a term that accounts for temporally autocorrelated environmental variability ($X(t)$). This variable is based on the following equation that includes terms that set the extent of autocorrelation (C_1), inherent variability (C_2), and the amplitude of the variability (C_3) in the system:

$$(8) \qquad X(t) = \overline{X} + \left\{ C_1 \cdot [X(t-1) - \overline{X}] + C_2 \cdot N \cdot \sqrt{1 - C_1^2} \right\} \cdot C_3$$

Here, $\overline{X}$ is the average value of the coefficient (chosen to be 0), and N is a random number drawn from a standard normal distribution $N(0,1)$. As an example, a 25-year period of the stochasticity term and the combined seasonality and stochasticity term is provided (Figs. 1*b*–1*c*). The initial setting for the stochasticity parameters creates low-frequency interannual variation such that unusually good or bad feeding conditions may persist for multiple years.

Cost of carrying energy stores

The model includes two sources of energetic costs required to maintain energy stores: the metabolic costs of maintaining store tissue and the influence of a change in body shape on the energy required for movement (hydrodynamics). This metabolic cost of carrying stores (C_{Stores}, kJ·month^{-1}) is a function of E_{Stores} (calculated within the parentheses on the right side of eq. 9) and is calculated as

$$C_{\text{Stores}}(E_{\text{Stores}}) = \tau \cdot (W_{\text{Total}}^{\lambda} - W_{\text{Structure}}^{\lambda}) \cdot H_{\text{Adj}}(K) \quad (9)$$

The value for τ implies that the mass-specific cost of maintenance of energy stores is less than the cost of maintaining other tissue because lipids are less metabolically active than somatic tissue. The exponent λ follows the allometric scaling of metabolic rate (Fitzgibbon et al. 2008), and H_{Adj} (unitless, ranging between 0 and 1) is the adjustment of metabolic costs resulting from the influence of energy stores, producing a more bulky appearance with less efficient hydrodynamics (Vogel 1994). The value for this adjustment is calculated as

$$H_{\text{Adj}}(K) = \left(\frac{K}{K_{\text{Min}}}\right)^{v} \quad (10)$$

where v (unitless) scales the increase in H_{Adj} with increasing values for K.

Energy allocation

Available energy is allocated between growth and energy storage at each time step (Roff 1983). The proportion of energy directed toward energy storage is u, which is a variable assigned at each time step in the model based on results from the optimizing algorithm portion of the model. The values of u and I determine the change in values for E_{Stores} and $W_{\text{Structure}}$ (and, consequently, L).

If I_{Net} is positive, then the energy that is available for tissue production is calculated as

$$E_{\text{Prod}} = I_{\text{Net}} \cdot C_{\text{s}} \quad (11)$$

where C_{s} is the proportion of assimilated energy required to synthesize new tissue (Wieser 1994). Energy available to production is then allocated to energy stores as

$$E_{\text{Stores}}(t+1|u) = E_{\text{Stores}}(t) + u \cdot E_{\text{Prod}} \quad (12)$$

and the change in $E_{\text{Structure}}$ as

$$E_{\text{Structure}}(t+1|u) = E_{\text{Structure}}(t) + (1-u) \cdot E_{\text{Prod}} \quad (13)$$

If I_{Net} is negative, then energy is drawn from energy stores to meet the net energy deficit as

$$E_{\text{Stores}}(t+1) = E_{\text{Stores}}(t) + I_{\text{Net}} \quad (14)$$

The value for $W_{\text{Structure}}(t+1)$ is calculated as

$$W_{\text{Structure}}(t+1) = \frac{E_{\text{Structure}}}{\rho_{\text{Structure}}} \quad (15)$$

where $\rho_{\text{Structure}}$ (kJ·g^{-1}) is the energy density of somatic tissue. The value for $W_{\text{Stores}}(t+1)$ is calculated based on eq. 2. A new value for $W_{\text{Total}}(t+1)$ is calculated from the values for $W_{\text{Structure}}(t+1)$ and $W_{\text{Stores}}(t+1)$ as in eq. 3. Based on the calculation for Fulton's condition factor $K = 100W \cdot L^{-3}$, the new length of the fish is calculated as

$$L(t+1) = \left[\frac{100 \cdot W_{\text{Structure}}(t+1)}{K_{\text{Min}}}\right]^{\frac{1}{3}} \quad (16)$$

Migration and spawning

Tagging studies find that large, presumably mature, ABFT have complex and varied movement patterns as they move between the feeding and potential spawning grounds (Block et al. 2005; Sibert et al. 2006; Galuardi et al.2010). Furthermore, little is known regarding the amount of feeding that occurs during migration and spawning, though based on depth patterns from electronic tags and stable isotope analysis (Estrada et al. 2005; Logan 2010), it is likely that ABFT feed during both. Regardless, movement between feeding and spawning areas requires time and energy expenditure. To simplify, time and energetic cost of migration and spawning is compartmentalized in discrete periods in the model. Note that time involves an opportunity cost, as the tuna cannot perform other activities while migrating or spawning, while the energetic cost has implications for energy stores required. Because of this, the model includes both time and energetic costs, and these are part of different trade-offs that are linked with size (size affects the energy costs of swimming and the timing of migration through swimming speed). The feeding and spawning areas themselves are not spatially explicit, yet the two areas are separated by a specified distance. We assumed that tuna spend time either in a feeding area or a spawning area or migrate between these two areas. For migration, ABFT make directed movements between the feeding and spawning areas based on an annual cycle driven by a spatially and temporally fixed spawning schedule, but may forage underway. Fish utilize a single spawning area, and spawning includes all behaviors and activity associated with spawning. Spawning occurs in May both in the Gulf of Mexico and the Mediterranean (Mather et al. 1995). The model allows for sufficient time for the fish to arrive on the spawning grounds by 1 May. Following spawning at the end of May, the fish return to the feeding area. The following calculations are used to determine the energetic cost of spawning and the amount of energy that is put towards egg production.

Migration time

The migration time (T_{Mig}, months) is a function of the distance between the feeding and spawning areas (D_{Mig}, m) and the speed that the fish travels during migration ($U_{\text{Opt}}(L)$, m·month^{-1}) and is calculated as

$$T_{\text{Mig}} = \frac{D_{\text{Mig}}}{U_{\text{Opt}}(L)} \quad (17)$$

The fish is assumed to travel at an optimal cruising speed according to

$$U_{\mathrm{Opt}} = r \cdot L^{e} \quad (18)$$

where parameters r and e are based on a relationship for pelagic fish (Ware 1978). As an example, migration speed and time are shown as a function of fish length (Fig. 2).

Migration costs

We assumed that the metabolic costs during migration scale according to the time required for migration and the physical power required for fish movement through the water column. The metabolic cost of migration to and from the spawning area is calculated as

$$C_{\mathrm{Mig}} = 2 \cdot T_{\mathrm{Mig}} \cdot \left(\alpha \cdot L^{\beta} \cdot U_{\mathrm{Opt}}^{\varepsilon}\right) \quad (19)$$

where β and ε (unitless) are scaling exponents drawn from a study of the relationship between fish length and power required for movement at an optimal cruising speed (Ware 1978). The coefficient α is tuned so that the metabolic cost is equivalent to twice the routine metabolic rate (see spawning metabolic rate calculation below) for a 200 cm fish. (Ware (1978) found that fish metabolic rate while swimming at an optimal speed was two times routine metabolic rate.) The factor 2 is to account for migration both ways.

Spawning costs

Metabolic costs for ABFT during spawning are unknown (Mather et al. 1995). Therefore, metabolic rate during spawning is estimated according to Fitzgibbon et al. (2008), who measured routine metabolic rate (RMR, kJ·month^{-1}) for non-spawning southern bluefin tuna (*Thunnus maccoyii*) in holding pens while traveling approximately 100 cm·s^{-1}:

$$\mathrm{RMR} = \varpi \cdot W_{\mathrm{Total}}^{\psi} \quad (20)$$

This metabolic rate during spawning was adjusted for temperature as follows:

$$\mathrm{RMR}_{\mathrm{TAdj}} = \mathrm{RMR} \cdot Q_{10}^{\frac{T_{\mathrm{w}} - 25}{10}} \quad (21)$$

where T_{w} is water temperature (°C). The value for Q_{10} is representative of the metabolic influence of temperature for fish (White et al. 2006) and was used by Fitzgibbon et al. (2008) for tuna species. The temperature-adjusted metabolic rate was then adjusted for activity (assumed to be 25% higher than temperature adjusted routine metabolic cost) during spawning, giving the metabolic cost of spawning (C_{Spawn}, kJ·month^{-1}):

$$C_{\mathrm{Spawn}} = \mathrm{RMR}_{\mathrm{TAdj}} \cdot \mathrm{Act} \quad (22)$$

Temperature is usually much higher on the spawning grounds than on the feeding grounds, particularly for W-BFT when in the Caribbean. Although temperature has a profound influence on physiological rates, tuna are known to make extensive vertical migrations to different temperature regimes during the spawning migration and to a lesser degree during spawning itself (Block et al. 2001). As their large body sizes may buffer temperature fluctuations in the shorter term, the overall effect of warmer surface waters on energetic costs is uncertain. Because the model does not include vertical migration behavior explicitly, we therefore choose $T_{\mathrm{w}} = 24$ °C, which is a typical temperature experienced by ABFT during spawning in the Gulf of Mexico (Mather et al. 1995; Garcia et al. 2005; Teo et al. 2007*a*).

Fig. 2. Migration time speed as it varies with fish length (L). Speed is shown in L·s^{-1} (solid line) and m·s^{-1} (dotted line).

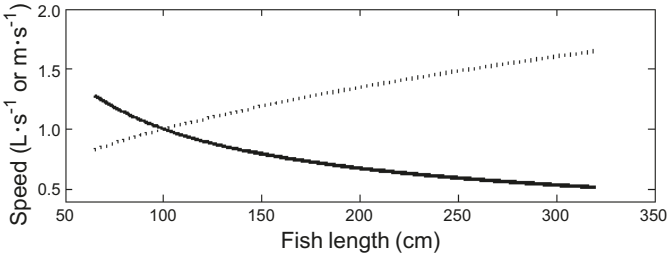

Intake while migrating and spawning

Although ABFT appear to feed sporadically during migration and spawning (Mather et al. 1995), we assumed that fish do not add to their energy stores during this period, but that feeding does occur and compensates for some proportion of metabolic costs during these activities. The total metabolic cost of migration and spawning (C_{MigSpawn}, kJ·month^{-1}) is then calculated as

$$C_{\mathrm{MigSpawn}} = (C_{\mathrm{Mig}} \cdot F_{\mathrm{Mig}}) + (C_{\mathrm{Spawn}} \cdot F_{\mathrm{Spawn}}) \quad (23)$$

where F_{Mig} (unitless) and F_{Spawn} (unitless) are the proportions of metabolic costs not met by feeding during migration and spawning (including activity but excluding gonads), respectively.

Energy to egg production

A spawning bluefin tuna preserves some of its stored energy to maintain survival. Therefore, spawning fish only use stored energy that will allow for the metabolic costs of migration and spawning and that will leave a fish in a particular condition upon return to the feeding ground ($K_{\mathrm{PostSpawn}}$, unitless). The remaining stored energy is spawned, and the energy put toward egg production (E_{Egg}, kJ) is calculated as

$$E_{\mathrm{Egg}} = \left[E_{\mathrm{StoresPreSpawn}} - C_{\mathrm{MigSpawn}} - \frac{(K_{\mathrm{PostSpawn}} - K_{\mathrm{Min}}) \cdot L^{3} \cdot \rho_{\mathrm{Stores}}}{100}\right] \cdot C_{\mathrm{s}} \quad (24)$$

where $E_{\mathrm{StoresPreSpawn}}$ (kJ) is the stored energy prior to migration and spawning. The efficiency of biosynthesis C_{s} is used again and represents the energetic cost of transforming stored fat and protein to eggs in the gonads. The factor 100 in the denominator is a conversion for Fulton condition when length is expressed in centimetres and mass in grams. We do not include larval growth and survival explicitly. Recruits are introduced at age 18 months, which implicitly assumes that mean survival from spawned egg to age 18 months does not vary systematically with the mother's phenotype or the environment in the model.

Mortality

A background mortality rate (M_c, year^{-1}) is imposed on fish evenly throughout the year regardless of its activity, so that survival probability (S_v, month^{-1}) is calculated as

$$S_v = \exp\left(\frac{-M_c}{12}\right) \quad (25)$$

In addition, fish that have a condition below a critical Fulton's K (K_{Min}) value die, such that $S_v = 0$.

We recognize that fish experience both natural and fishing mortalities, and mortality may vary with size, age, or whether a fish is spawning, migrating, or in a feeding area. Furthermore, modeling has suggested that where and when mortality occurs is important for influencing emerging population characteristics such as growth, age-at-maturity, and reproductive effort (Law and Grey 1989; Dunlop et al. 2009). However, a simple, integrated mortality term was used in this study because of a lack of extensive data on variability in natural and fishing mortality. An additive approach to this term would have introduced further unknown parameters and was not required based on the objectives of this study.

Optimizing algorithm

Dynamic programming is used to optimize life history strategies (Houston and McNamara 1999; Clark and Mangel 2000), which produces a "decision map" that guides energy allocation and the decision to spawn based on individual state values in the forward simulations (see next section: "Forward simulations: initialization and exploratory scenarios"). This approach begins at a maximum age (when all fish die from senescence and future reproductive success is assumed to be zero) and, working backwards in time, optimizes the allocation of energy to somatic growth versus energy stores (for reproduction or survival during low prey availability). As a fitness measure, the model maximizes expected lifetime egg production. The maximum age used in this study is 25 years, and the maximum size was set at 350 cm. Although older ABFT have been observed (Neilson and Campana 2008), a 25-year maximum age was used because of the scarcity of fish older than this age (Mather et al. 1995). The optimization problem then finds the energy allocation (u) for each combination of variables that are available to the individual (state variables: age a, body length L, stored energy E, food environment ϕ) that maximizes expected future reproductive output (V) at each decision point:

$$V(a, L, E, \phi) = \max_u \left\{ b(E) + S \sum_{\phi(t+1)} P[\phi(t+1)|\phi(t)] \times V[a+1, L(t+1|u), E(t+1|u), \phi(t+1)] \right\} \quad (26)$$

Here, $b(E)$ is the fecundity when spawned, S is survivorship, and $P[\phi(t+1)\,|\,\phi(t)]$ is the probability of realizing a food environment in the next time step, given the value of the food environment in the current time step. $L(t+1\,|\,u)$ and $E(t+1\,|\,u)$ are the new states in the next time step, depending on the energy allocation u. If the individual survives, its future expected reproductive value is then given by $V[a+1, L(t+1\,|\,u), E(t+1\,|\,u), \phi(t+1)]$.

Two additional optimizations are made during the backwards iteration. First, the postspawning condition ($K_{PostSpawn}$) that produces the maximum expected future egg production is calculated during the spawning period for each combination of state variables. The optimal postspawning condition depends on a balance between benefits gained from investment in a current reproductive effort and those gained by increased future survival and reproduction (as a result of preserving greater energy reserves when returning to the feeding area the following season). Second, during the spawning period, the fitness value for both spawning and nonspawning are calculated and the behavior that maximizes fitness is recorded for each combination of state variables. When fish do not spawn, they produce no eggs, but are able to allocate energy to growth and do not incur the energetic costs of migration and spawning.

Overall, the optimizing algorithm produces a life history plan that guides (*i*) allocation of energy, (*ii*) the decision to spawn, and (*iii*) postspawning condition as a function of each combination of state variables during the forward simulation. The critical assumption here is that individuals, either through selection or through phenotypic plasticity, behave optimally regarding these three decision sets as they interact with a particular environmental scenario.

Forward simulations: initialization and exploratory scenarios

Forward simulations of the model begin for age class 1 (year) fish in January (approximately 18 months) at a size of 65 cm (see Mather et al. 1995) and a Fulton's K of 1.5. The forward simulation was run for a 2000-year period under each environmental scenario. Such a long simulation is needed to record the mean and variability of the response in that environment, as averaging over time is the same as averaging over environments when the environment is fluctuating around an equilibrium. Fish were allowed to skip spawning in any given year, and age-at-maturity was defined as the age that fish first spawn. Population characteristics were recorded during the second 1000 years of simulations, thus allowing for the model to stabilize during the first 1000 years. A parameter space for a reference scenario (baseline values in Tables 1–3) was selected to facilitate validation of the model through comparison of model output with observations of growth (Turner and Restrepo 1994; Neilson and Campana 2008; Restrepo et al. 2010), age-at-maturity (Turner et al. 1991; Goldstein et al. 2007), and seasonal changes in condition (W. Golet and M. Lutcavage, unpublished data) for W-BFT. We then use the model to test whether the population characteristics can be altered to match those of E-BFT by increasing mortality and decreasing migratory costs. In place of a potentially overwhelming set of sensitivity studies involving all parameters, a subset of primary sensitivity simulations were carried out with parameters that are central to the model and may vary among ABFT subpopulations (Table 2). These simulations were designed to give insight into the sensitivity of the model to variability among uncertain parameters while providing some insight into factors that may be responsible for observed variability in life history patterns among ABFT subpopulations. These simulation sets investigated the influence of variability among mortality rate and spawning migration distance, expressed as the proportion of energetic costs

Table 1. Parameters used in the Atlantic bluefin tuna life history model.

Symbol	Definition	Value and unit	Source
K_{Min}	Minimum value for Fulton's K	1.4 (unitless)	W. Golet and M. Lutcavage, unpublished data
K_{Max}	Maximum value for Fulton's K	2.1 (unitless)	W. Golet and M. Lutcavage, unpublished data
ρ_{Stores}	Wet mass energy density of stored lipids	8.7×10^6 kJ·kg^{-1}	Assumed similar to *Gadus morhua*; Jørgensen and Fiksen 2006
$\rho_{Structure}$	Wet mass energy density of somatic tissue	4.2×10^6 kJ·kg^{-1}	Assumed similar to *Gadus morhua*; Holdway and Beamish 1984
b	Scaling of the intake calculation	2.4 (unitless)	Overholtz 2006; Fitzgibbon et al. 2008
S_{Mean}	Mean value of seasonality over a year	0.65 (unitless)	Set by fitting seasonal growth to observations; see Fig. 3*b*
$\overline{X}$	Mean value for stochasticity (X)	0.0 (unitless)	Tuned to give interindividual variability that fits reasonably well with observations
C_2	Variance in stochasticity (X)	0.4 (unitless)	
C_3	Scaling of stochasticity (X)	0.4 (unitless)	
λ	Scaling of metabolic cost of energy stores	0.86 (unitless)	Fitzgibbon et al. 2008
S_y	Cost of biosynthesis	0.77 (unitless)	Wieser 1994
r	Coefficient for calculation of optimal cruising swim speed	0.138 s^{-1}	Ware 1978
e	Scaling factor for calculation of optimal cruising swim speed	0.43 (unitless)	Ware 1978
β	Scaling with length of cost of migration	1.42 unitless	Ware 1978
ε	Scaling with swim speed of cost of migration	2.42 unitless	Ware 1978
ϖ	Coefficient for RMR calculation	4.08×10^6 kJ·month^{-1}	Fitzgibbon et al. 2008
ψ	Scaling of RMR with total mass	0.89 (unitless)	Fitzgibbon et al. 2008
Q_{10}	Scaling of metabolic rate with temperature (at temperature of 25 °C)	1.67 (unitless)	White et al. 2006
T_w	Water temperature experienced during spawning	24 °C	Mather et al. 1995; Garcia et al. 2005; Teo et al. 2007*a*
—	Spawning month	May	Mather et al. 1995

Note: RMR, routine metabolic rate.

Table 2. Parameters varied in primary sensitivity simulations of the Atlantic bluefin tuna life history model.

Parameter	Definition	Baseline: sensitivity range	Rationale for values
M	Annual mortality rate	0.34: 0.10 to 0.45 (year^{-1})	Natural mortality (ICCAT 2007) plus variable fishing mortality
D_{Mig}	Migration distance	3500: 500 to 4500 (km)	Mather et al. 1995; Block et al. 2001, 2005; Galuardi et al. 2010
F_{Mig}	Proportion of metabolic cost during migration that is compensated for by feeding	0.025: 0.15 to 0.01 (unitless)	Tuned to allow survival and to match observed growth and maturity schedules
F_{Spawn}	Proportion of metabolic cost during spawning (excluding energy to gonads) that is compensated for by feeding		

Note: Exploratory range and the baseline value are given. Sources are indicated where applicable; otherwise, rationale or method for choice is given. Results provided in Figs. 8 and 9.

covered by feeding during migration and spawning (Table 2). We selected the range of integrated mortality rate to encompass an estimated natural mortality (0.10 to 0.24 year^{-1}; ICCAT 2007, 2009) plus reasonable fishing mortality (bringing total morality to 0.45 year^{-1}). The range of migratory distances used in these simulations encompass shorter spawning migrations that have been observed for E-BFT (500–1000 km; Mather et al. 1995; Block et al. 2005) and longer migrations recorded for W-BFT (3500 km; Block et al. 2001, 2005; Galuardi et al. 2010). The influence of variability in the proportion of metabolic costs incurred during migration and spawning on population characteristics were conducted over a range of plausible values. Secondary sensitivity simulations were carried out for additional poorly constrained parameters (Table 3), again over a range of plausible values.

Results

Model validation and reference simulation

The model's reference simulation produced indeterminate growth, with the fastest growth rate during the fish's first 8 years (Fig. 3*a*). Growth rate is then reduced before reaching an asymptote at around 275 cm when fish are >21 years. For fish >15 years, the simulated fish are smaller than is predicted by the W-BFT growth curve and slightly larger than is predicted according to the E-BFT growth curve. However, the size-at-age curve for W-BFT is uncertain, and the modeled size-at-age values for older fish are slightly larger than data from a recent study that aged W-BFT (Neilson and Campana 2008; Restrepo et al. 2010). Juvenile growth follows a seasonal pattern similar to that observed in W-BFT

Table 3. Parameters varied in secondary sensitivity simulations of the Atlantic bluefin tuna life history model.

Parameter	Definition	Sensitivity range (baseline: range)	Rationale for baseline values	Effect of parameter increase on growth	Effect of parameter increase on maturity schedule
Act	Spawning activity adjustment	1.25: 0.625–1.875 (unitless)	To allow for increased behavioral activity during mating and spawning	Slight decrease	Slight delay in maturity
a	Intake coefficient	1.8: 1.62–1.98 (unitless)	Set to match observed growth and condition changes	Increase	Slight delay in maturity
τ	Coefficient for metabolic cost of energy stores	3.16×10^4: $1.58–4.75\times10^4$ ($kJ\cdot kg^{-1}\cdot month^{-1}$)	Set lower than for somatic tissue, as stored lipids generally are less metabolically active	Increase	Delayed maturity
v	Scaling of the hydrodynamic cost of energy stores	2.0: 1.0–3.0 (unitless)	Drag scales as cross-sectional area (Vogel 1994); this exponent assumes further efficiency loss at higher condition factors	Increase to 14 years, then decrease	Slightly earlier maturity
S_{Amp}	Seasonality amplitude (maximum value)	0.35: 0.175–0.525 (unitless)	Set by fitting seasonal growth to observations; see Fig. 3*b*	Increase	Delayed maturity
D_{Peak}	Seasonality peak (timing)	15 Aug.: 1 Aug. – 1 Sept.	Maximum seasonal mass gain; W. Golet and M. Lutcavage, unpublished data	(Later peak) decrease to 12 years, then increase	(Later peak) earlier maturity
C_1	Autocorrelation	0.90: 0.30–0.99 (unitless)	Tuned to give interindividual variability that fits reasonably well with observations	Slight increase	Slightly earlier maturity
α	Coefficient for cost of migration	6.51×10^4: $1.30–1.17\times10^4$ ($kJ\cdot m^{-2}$)	Tuned to be twice RMR for a 200 cm fish; see also Ware 1978	Little change	Delayed maturity

Note: These parameters were chosen because of uncertainty over their values. Sources are indicated where applicable, otherwise rationale or method for choice of baseline parameter value is given. Results are summarized below and presented in Appendix A, Fig. A1.

(Fig. 3*b*). The observed mean monthly W-BFT Fulton's K between May and November for mature fish compares favorably with increases in condition over the same time period produced by the model (Fig. 3*c*). Older, mature fish maintained a higher Fulton's K during the year, largely because a higher U_{Opt} allowed them to arrive on the feeding grounds earlier in the year to recover stores lost during migration and spawning. Juvenile fish allocated energy primarily to growth and allocated to energy stores only to maintain a stable Fulton's K value of around 1.54 throughout the year. Under reference conditions, fish matured between the ages of 6 and 11 years (150–235 cm), with age at 50% maturity at 8 years (210 cm) (Fig. 3*c*). The size- and age-at-maturity under the reference conditions were within the range of estimations based on field data and were more similar to estimates of the maturity schedule for W-BFT (7–10 years; Turner et al. 1991; Goldstein et al. 2007) than for E-BFT (3–5 years; Tiews 1963; Medina et al. 2002; Corriero et al. 2005).

To demonstrate the evolution of an individual life trajectory under reference conditions, fish length, food environment, condition, fish mass, energy in egg production, and allocation of energy during a 25-year lifespan are shown (Fig. 4). This particular fish began spawning in its ninth year when it was 200 cm and demonstrated a seasonal and maturation-stage pattern in energy allocation (Fig. 4*f*). During the juvenile period, this fish allocated energy primarily toward growth, with seasonal increase in energy directed to storage in winter when net energy intake is low. After maturation, the adult fish primarily favored energy storage, with a brief period of partial energy allocation to growth immediately following return from the spawning grounds.

Skipped spawning

Under reference conditions, skipped spawning occurred primarily among younger, recently matured fish. The proportion of individuals that skipped spawning decreased quickly with age from age 7 (the first opportunity for skipped spawning) to 13 years, and no fish older than 13 years skipped spawning (Fig. 5*a*). Under the reference conditions, 42% of fish spawned during their eighth year. In comparison with these, skipped spawners were in lower condition, weighed less, and were shorter just prior to migration (Figs. 5*b*–5*d*).

The mean growth curve was strongly influenced by the age-at-maturity schedule. In general, mean growth curves exhibit a reduced rate of growth following maturity as those fish begin to allocate energy to both growth and reproduction rather than solely to growth. This results in a reduced size at a particular age for an earlier maturing fish population, but only after some proportion of that population matures (Fig. 6).

Eastern bluefin tuna

To shift the reference simulation that resembled population characteristics of W-BFT to those of E-BFT, it was necessary to (*i*) reduce the reproductive costs by reducing the migration

Fig. 3. (*a*) Comparison of length-at-age from model output (mean and standard error) for the reference scenario (solid line) with growth data from the western Atlantic from Neilson and Campana (2008) (open circles) and the ICCAT growth curves for W-BFT (dot-dashed line) and E-BFT (dotted line). (*b*) Juvenile growth predicted by the model (open circles, with standard error) and based on data from the western North Atlantic (Mather and Shuck 1960; solid line = data; dotted line = interpolation). (*c*) Model output for the reference condition for monthly mean Fulton's *K* condition index for 10- (solid line), 18- (dot-dashed line), and 24- (dashed line) year-old fish and mean monthly value of Fulton's *K* for fish between 8- and 20+-year-old fish in the Gulf of Maine (dotted line) between June and November from catch data between 1984 and 2007. (*d*) The proportion of spawning individuals as a function of age (top) and size (bottom) produced through 1000 simulations of the model under reference conditions. The current estimates of age- and size-at-maturity for E-BFT and W-BFT are indicated.

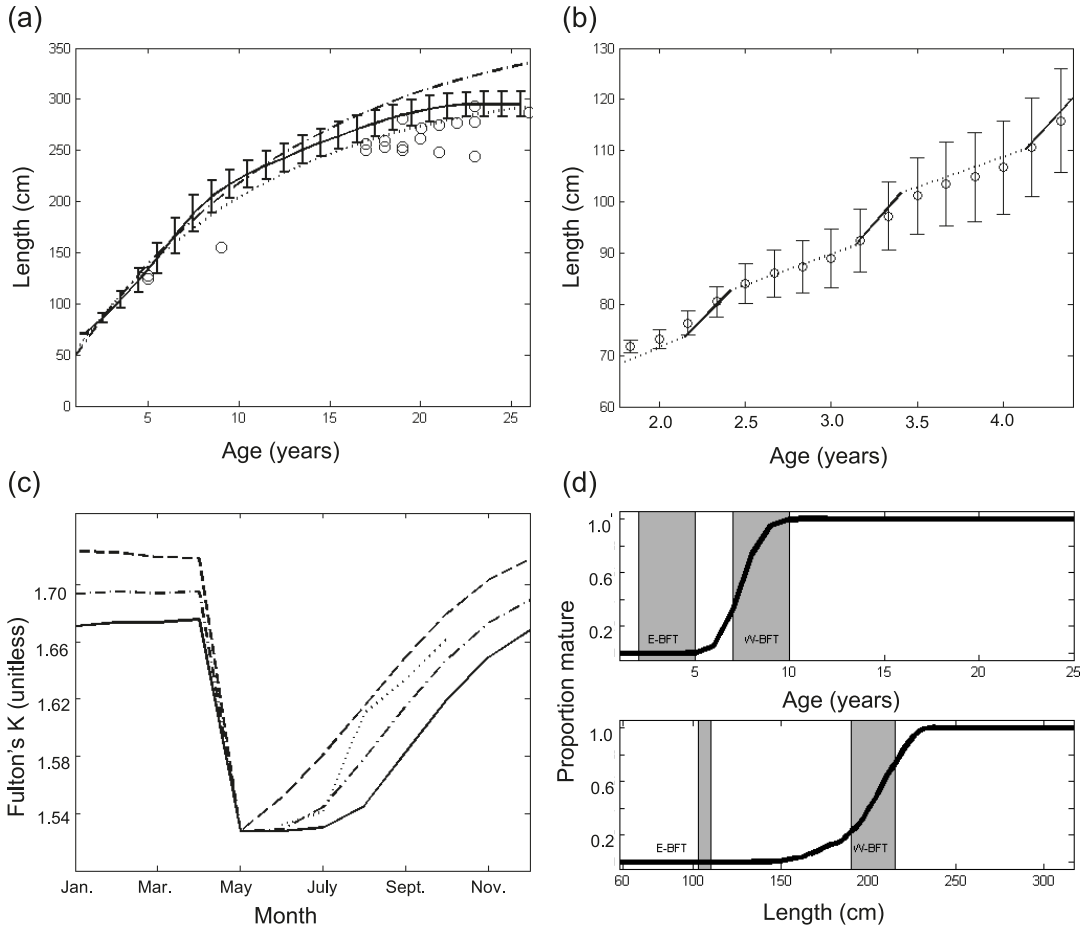

distance (from 3500 to 500 km) and increase the proportion metabolic costs met by feeding during spawning and migration (from 0.985 to 0.995) and (*ii*) increase the mortality rate to 0.37. This produced a growth curve (Fig. 7*a*) and age-at-maturity (Fig. 7*b*) similar to what is currently accepted for E-BFT. Length at 50% maturity was similar to that which is accepted for E-BFT (Fig. 7*b*), though maturity occurs over a broad range of lengths (70–170 cm) and does not increase linearly over that range. Instead, local peaks in proportion spawning occur over this length range. This pattern reflects that only the largest fish within the youngest age classes are spawning. The compounding effects of environmental stochasticity smooth these peaks as fish age and age classes increasingly overlap in length. As was the case for the W-BFT conditions, skipped spawning occurs only for the youngest recently matured fish (ages 3 to 5 years; Fig. 7*c*).

Sensitivity analyses

The age at 50% maturity ranged between 13 and 3 years as annual mortality rate was varied between 0.1 and 0.45 (year^{-1}), and the spawning migration distance was varied between 500 and 4500 km (Fig. 8). Over this range of variability, the age at 50% maturity decreases as annual mortality rate increases and increases with increasing spawning migration distance. The same range in mortality rate, combined with the proportion of metabolic costs met by feeding during migration and spawning (ranging between 0.975 and 1.000), produced an age at 50% maturity between 4 and 14 years (Fig. 9). (Results for the secondary sensitivity simulations are summarized in Table 3 and are included in Appendix A.)

Discussion

The reference simulation recreates observations of growth, age-at-maturity, and seasonal variability in condition for W-BFT, although we acknowledge that their maturity and reproduction schedules are not well known. This suggests that the model structure and parameter settings provide information necessary to adequately represent the interaction between the environment and ABFT life history. This gives us confidence in the model structure and parameterizations and allows us to

Fig. 4. An individual example of fish length (*a*), food environment (*b*), condition (*c*), mass (*d*), energy put toward eggs (*e*), and the proportion of energy allocation to energy stores (*f*; no values are plotted when there is no ingested energy to allocate, e.g., during spawning) over the 25-year life of a BFT under reference conditions in the model.

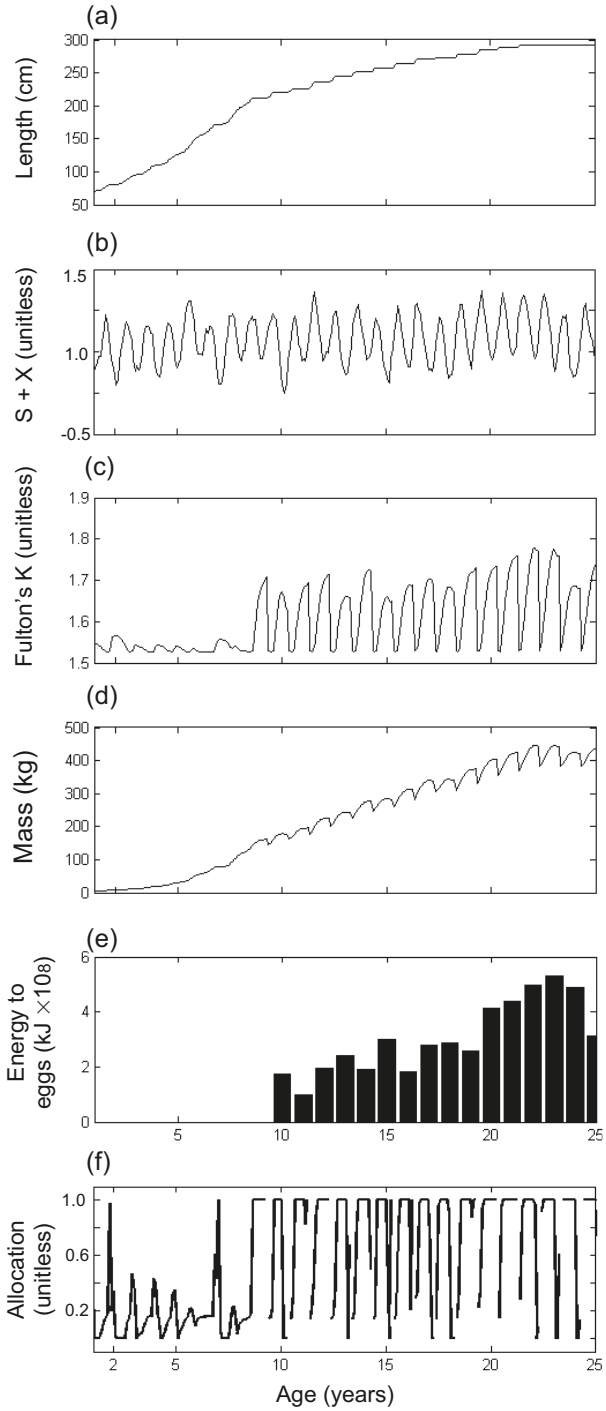

explore and discuss some of the model components and parameters that are important for model behavior.

Net energy intake and seasonality

While integration of ingested energy and metabolic costs into net energy intake limited the ability of the model to resolve differences in specific sources of environmental variability (e.g., prey quality, cost of foraging), we avoided major difficulties by using this approach. ABFT have extremely high energy demands, requiring equally high energy intake rates. Therefore, energy available for allocation to growth and energy stores is the difference between two values that are extremely difficult to estimate, and using an additive approach to calculate net energy intake made it difficult to achieve stable model dynamics. The simplifying assumption of an integrated net energy intake function allowed for more stable model behavior and allowed us to easily add seasonality to the model. Given the uncertainty and complexity in food quality, abundance, and metabolic rate over a bluefin's lifespan, this was highly desirable.

The seasonality function is a central component of the model that is responsible for accurately predicting juvenile growth and the increase in fat stores for larger adults during the summer and autumn feeding period. It is also a critical process in determining age-at-maturity because the benefit of migration and spawning is weighed against the benefits associated with feeding opportunities missed while migrating and spawning, which are inherent to the seasonality function. Spawning (May) occurs just after the net energy intake is at its lowest value (March), and the return migration in June and July occur as the seasonality function is increasing toward its August peak. Larger fish, because they are faster swimmers, are able to return to productive waters earlier and thus are able to capitalize on the increasingly favorable food conditions there. This represents an incentive for allocation to growth (along with increased ability to ingest and store energy), and the strength of this incentive varies with the phenology of peak seasonal energy intake. When this seasonality peaks earlier than 15 August, the incentive for growth is greater and age-at-maturity is delayed because larger fish are able to return from spawning to capitalize on earlier peak in seasonality. When seasonality peaks later, the incentive for growth is reduced, and age-at-maturity is younger because extended migration time for smaller fish does not influence their access to peak seasonality in energy intake. This highlights the importance of phenology and the complex costs and benefits linked to the timing of migration with respect to missed feeding opportunities.

Seasonality and environmental stochasticity were responsible for the postspawning condition having minimal or low variability in the simulations. This result reflects a poor correlation between the food environment immediately prior to and following migration and spawning, leaving ABFT unable to anticipate the food environment following spawning. This could also indicate that ABFT experience a relatively high and increasing net energy intake when they return to the feeding grounds and thus would not draw on their energy reserves. Therefore, we expect that higher optimal postspawning condition could result if fish experience lower forage quality upon their return to the feeding area (risking starvation) or if there is lower autocorrelation in the food environment (preventing fish from anticipating the food environment when they return to the feeding area based on conditions when they left for spawning).

Feeding during migration and spawning

The model is sensitive to the proportion of metabolic costs

Fig. 5. The rate that mature fish skip spawning (*a*) and the mean and standard deviation of Fulton's *K* (*b*), fish weight (*c*), and length (*d*) in March (month when spawning decision is made) for fish that spawn and those that do not spawn in their eighth year.

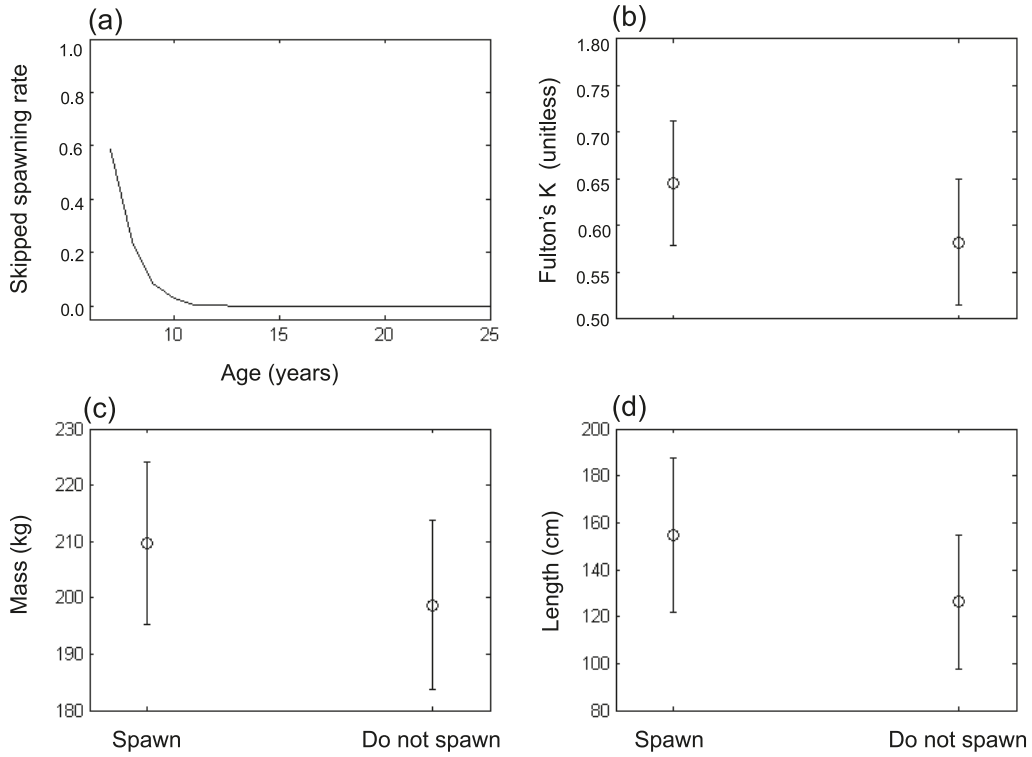

Fig. 6. Difference in growth for fish with a migration distance of 2500 km and age at 50% maturity of 4 years (dot-dashed line, mortality = 0.45) and 8 years (dotted line, mortality = 0.33). The remaining parameters are set at reference values.

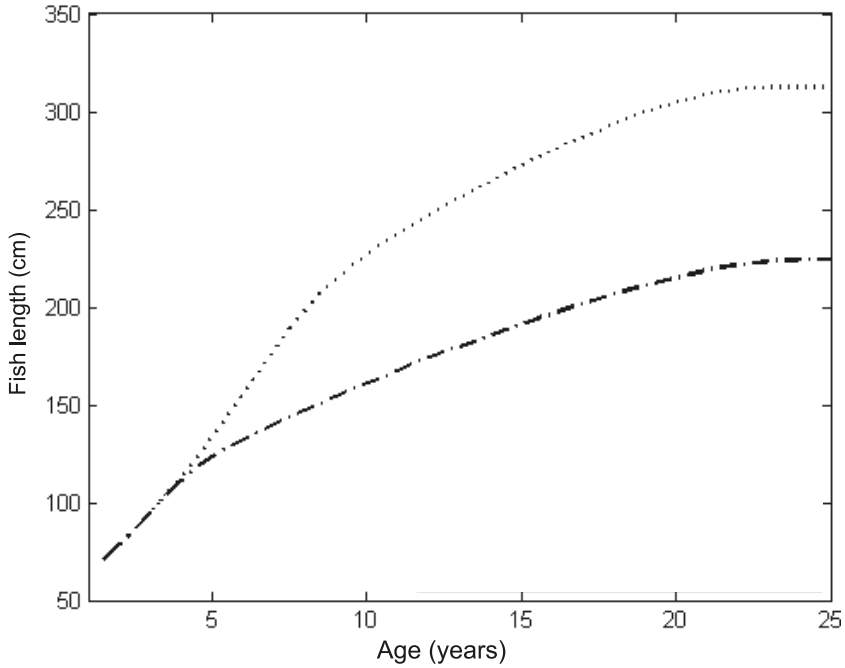

during migration and spawning that are covered by feeding. Large-scale migration presumably links individuals with habitat that is beneficial for an incipient developmental stage (e.g., migration between spawning and nursery habitats) or for larval development and survival (spawning migrations). Complex trade-offs should structure ABFT migration that balances benefits to larvae (e.g., food availability, lack of predators, favorable temperatures for growth) or adult condition with costs incurred by migrating and spawning (e.g., lack of food, thermal stress).

ABFT larval habitat requirements are not completely understood, though evidence suggests that most larvae re-

Fig. 7. (*a*) Comparison of length-at-age from model output (mean and standard error) for the scenario for E-BFT (solid line) with the ICCAT growth curves for W-BFT (dotted line) and E-BFT (dot-dashed line). (*b*) The proportion of spawning individuals as a function of age (top) and size (bottom) produced through 1000 simulations of the model under a possible E-BFT scenario. The current estimates of age- and size-at-maturity for E-BFT and W-BFT are indicated. (*c*) The rate that mature fish skip spawning for the E-BFT scenario.

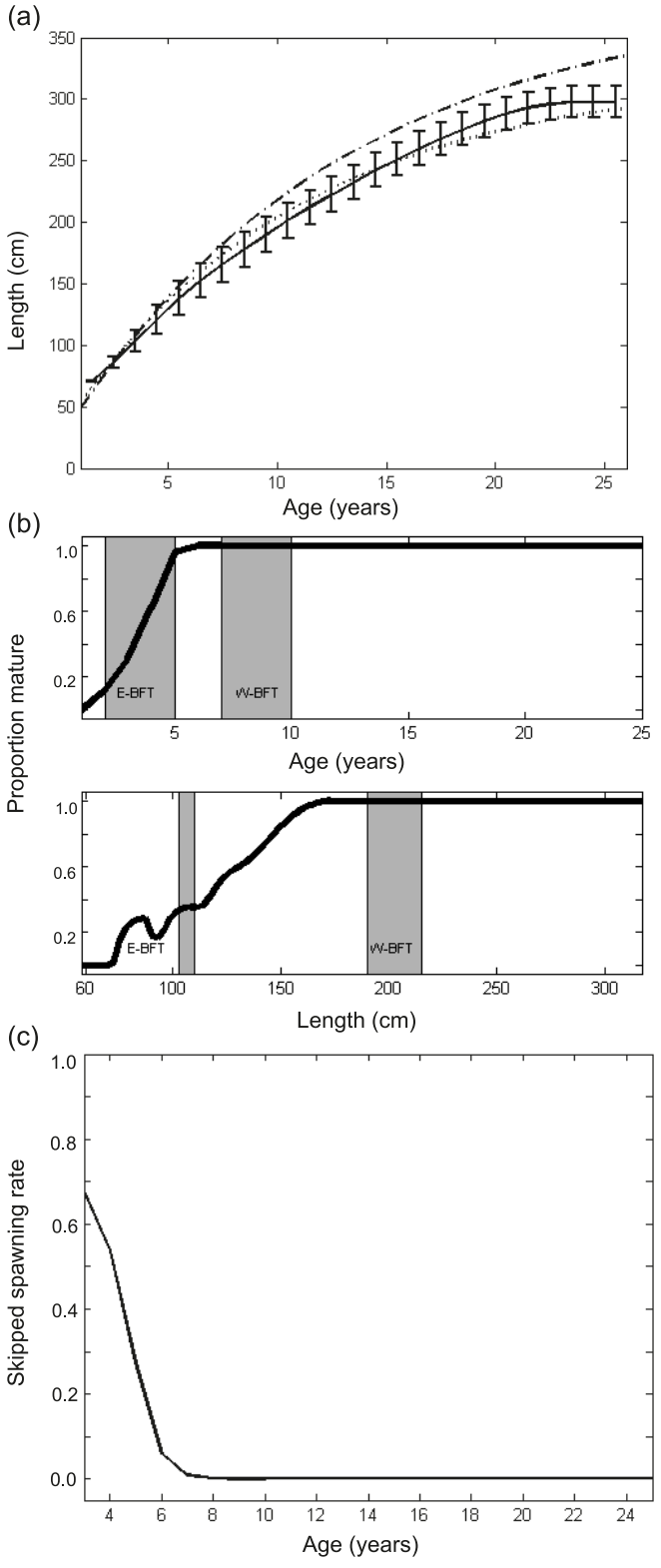

Fig. 8. The influence of variability in the spawning migration distance and cumulative annual mortality rate on age-at-maturity (50%).

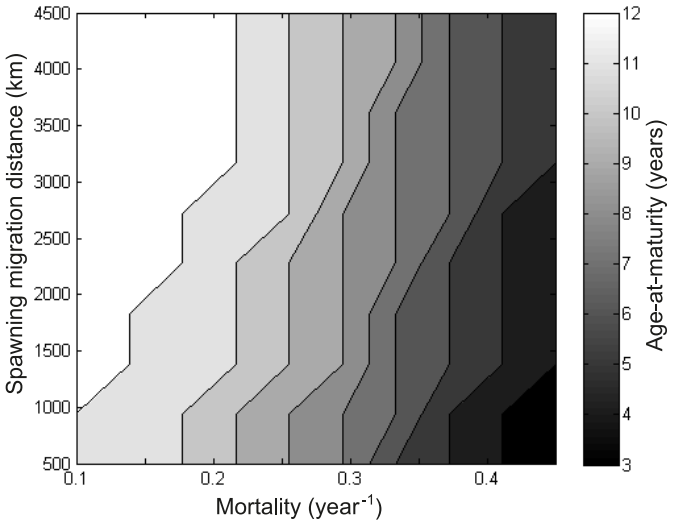

Fig. 9. The influence of variability in the proportion of metabolic costs met through feeding during a 3500 km migration and spawning and cumulative annual mortality rate on age-at-maturity (50%).

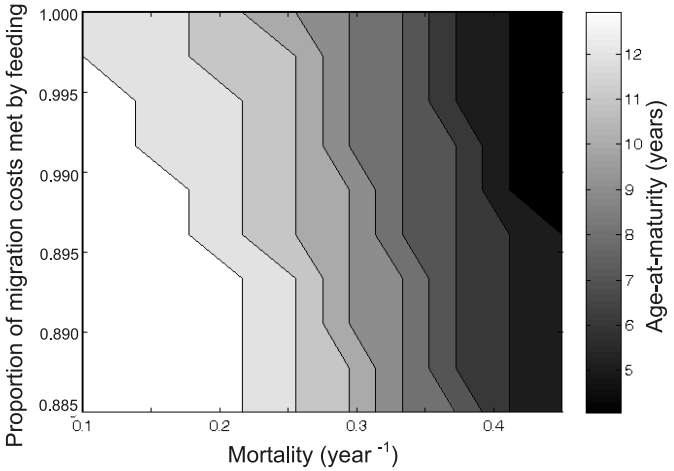

quire temperatures of at least 24 °C (Mather et al. 1995; Garcia et al. 2005). Although appropriate temperatures are necessary for larval development, the distribution and quality of food and predator density are also crucial factors. Improving our understanding of the complex interactions among factors influencing early life history that combine to determine the spatial and temporal variability of suitable spawning habitat (e.g., Lehodey et al. 2008) must be accomplished in future modeling efforts.

From the perspective of the adult, spawning areas are up to 20 °C warmer than their primary feeding areas (possibly introducing thermoregulatory stress), and their suitability as forage grounds for adult ABFT is not known. Uncertainty regarding adult migration and spawning energy requirements, thermal stresses, and feeding activity further limits our understanding of factors that structure trade-offs responsible for ABFT spawning habitat distributions and migration behaviors, though some studies have been able to provide relevant information on this topic.

For example, Pacific bluefin tuna (*Thunnus orientalis*) mi-

grate 8000 km from the western to the eastern Pacific during their first and second year along the Subarctic Frontal Zone (Inagake et al. 2001; Kitagawa et al. 2009), a behavior that may provide a beneficial thermal environment with high prey availability during migration (Kitagawa et al. 2009). Similar strategies for migrating ABFT are not well studied, although juveniles from 1–2 years make trans-Atlantic crossings (Mather et al. 1995) For W-BFT that migrate to the Gulf of Mexico during the putative breeding period, Teo et al. (2007*b*) found a directed movement pattern during migration away from summer feeding areas, suggesting a strategy that minimizes travel time and allows for only opportunistic feeding along the way. However, Galuardi et al. (2010) demonstrate complex and varied movement patterns (e.g., varied departure time from feeding areas, significant nondirected movement during migration, and varied residency periods within and outside of the Gulf of Mexico during the putative spawning period) of adult ABFT in the western Atlantic, suggesting more substantial feeding during the migration and spawning periods and possibly alternative spawning areas or frequent skipped spawning. Overall, little is known about migration strategies and the change in condition of ABFT following the presumed peak feeding and spawning periods.

Behaviors relevant to ABFT energy balance during the spawning period are also not well understood. Teo et al. (2007*b*) speculated that vertical movements in the Gulf of Mexico during the presumed spawning period reflect thermoregulatory and spawning behaviors, but they were not able to definitively identify feeding and spawning behaviors with electronic tags. The presence of ABFT in the Mediterranean year-round and in the Gulf of Mexico in early winter, well outside of the putative spawning period (Galuardi et al. 2010), suggest that spawning habitat is also productive foraging habitat. Stomach content analyses in the Mediterranean during the putative breeding period are inconclusive, but generally suggest that feeding is substantially reduced, particularly during spawning migrations (see references in Mather et al. 1995). The high energy requirements for ABFT, particularly during migration and spawning, coupled with observations including stomach contents and depth behaviors documented by electronic tags, suggest that considerable feeding occurs during this time.

In our model, we greatly simplified the costs associated with migration and spawning by using the amount of feeding that occurs during migration and spawning and the spawning migration distance. In reality, spawning cost may include additional factors such as increased mortality due to thermoregulatory stress and reduced oxygen or food availability. Regardless, the parameters chosen to represent the cost of migration and spawning, particularly the amount of feeding during migration and spawning, are extremely important for shaping the optimal ABFT life history strategy. Given this result and the complexity of observed ABFT migration behaviors (Galuardi et al. 2010), a topic for future research is to investigate specific migration activities (e.g., feeding, minimizing energy expenditure) and concurrent changes in physiology and condition during migration and spawning. Deployment of electronic tags such as the Daily Diary Tag (see Gleiss et al. 2009) with sensors capable of identifying feeding behavior, spawning, and metabolic rate will be particularly important to this effort. This work would improve our understanding of the processes that determine migration and spawning behavior — critical components of the ABFT life history that link with ABFT resiliency to habitat change and fishing pressures.

Skipped spawning

Deferred spawning after initial maturation is a behavior that represents a trade-off between immediate and anticipated future reproduction (Jørgensen et al. 2006), which has been observed in moderately long-lived fish species (Rideout et al. 2005), but has not been resolved for ABFT (Rooker et al. 2007). The presence of large, presumably mature fish outside of the Gulf of Mexico during the spawning period (Lutcavage et al. 1999; Block et al. 2005; Galuardi et al. 2010) may indicate that some ABFT skip spawning. If ABFT do omit spawning, this would also influence stock assessment and quota-setting calculations (Secor 2007). The simulations suggest that given the cost of migration (distance covered and the proportion of metabolic costs met during migration) and the single-spawning location assumption of the reference scenario, skipped spawning emerges as reproductive strategy that in some cases optimizes life-long fecundity. However, the model suggests that if skipped spawning is to occur, it would be most likely observed in younger fish that have recently matured. This agrees with results from a modeling study that found skipped spawning to be more common among young Atlantic cod (Jørgensen et al. 2006). However, Galuardi et al. (2010) found presumably older, large fish outside of known spawning areas during the period when spawning typically occurs. These fish were either skipping reproduction or spawning at unknown spawning locations. Our results suggest that skipped spawning is not likely to be an important strategy for older, mature fish and that the larger fish observed by Galuardi et al. (2010) away from spawning areas during the spawning period may have been selecting alternative, perhaps lower-quality spawning habitats. Alternatively, the model may be missing a critical process that would otherwise explain skipped spawning in older fish. A firm verdict on the question of skipped spawning in ABFT awaits results from reproductive physiology and maturity studies conducted in both ABFT feeding and spawning grounds.

Differences between eastern and western bluefin tuna

Results from this study also show that conditions that support differences in age-at-maturity generally result in very different growth curves — a pattern that emerges from differing age-specific allocation to reproduction and growth. However, it is also important to recognize that similar growth curves can reflect very different life histories. Restrepo et al. (2010) have recently proposed an improved growth curve for W-BFT that is similar to the currently accepted growth curve for E-BFT. If we accept that fish that spawn primarily in the Mediterranean or Gulf of Mexico mature at different ages, and that despite these differences, E-BFT and W-BFT have similar growth curves, we can consider whether differences in environmental conditions are responsible for this pattern. Although additional combinations may produce the same result, we provide one potential explanation for observed differences in W-BFT and E-BFT life histories; W-BFT experience lower mortality and increased migration and spawning costs

compared with E-BFT. This is in concordance with observations that suggest that spawning grounds in the Gulf of Mexico may be further from the feeding grounds than is the case for the Mediterranean. However, results from electronic tagging and microchemical analysis are inconclusive regarding the relative cost of migration for E-BFT vs. W-BFT. This presents an opportunity for future work in this area. Also, fishing in the Mediterranean has been ongoing for more than 1000 years (Fromentin and Powers 2005), and this higher mortality could have led to life history adaptations. However, mortality exclusively on mature individuals is generally expected to delay maturation (Law and Grey 1989), so a higher mortality would need to also affect juveniles and adolescents if it were to explain the observed differences between E-BFT and W-BFT.

Future model development

The model used in this study is a general one, and its structure could be changed to address additional questions. For example, the current model assumes a single spawning region that limits individuals to natal homing behavior. However, size-class frequency data of Pacific bluefin tuna (Itoh 2006) and ABFT in the Mediterranean (Heinisch et al. 2008) suggests that bluefin tuna may use different spawning sites at different times as they grow (enhanced spawning behavior plasticity). In addition, repeat homing and schooling behavior, where younger individuals learn successful migration behavior from older fish, has also been proposed (Fromentin and Powers 2005). Differences in spawning migration behavior such as these can influence the optimal life history strategy (Jørgensen et al. 2008), so future work could involve expanding the current model structure to include multiple spawning areas and alternative spawning behaviors. In addition, as we learn more about the distribution of habitat that is suitable for development of viable ABFT larvae, variability in the quality of spawning habitats can be incorporated into the modeling structure. In addition, ABFT can use multiple feeding areas (Fromentin and Powers 2005; Sibert et al. 2006; Walli et al. 2009) within years and over longer time periods, so future model development could be used to investigate trade-offs that determine optimal decisions for selecting foraging sites characterized by different seasonality in food quality and availability and distance from spawning habitat. Finally, in recent decades, fishing mortality experienced by E-BFT occurs in both the spawning and feeding areas, while W-BFT experience fishing mortality primarily in the feeding area (Fromentin and Powers 2005). Based on model studies, the location of fishing mortality (spawning vs. feeding grounds) can influence the optimal age-at-maturity and growth for a migratory species (Dunlop et al. 2009). The influence of variability in the location and size structure of fishing mortality can be explored with a simple extension of this model.

For the future, it might also be interesting to make a similar model that would allow other fitness measures. State-dependent dynamic programming models allow rich state dependence but require that the optimization criterion is the same over the course of optimization (in our case, expected lifetime reproductive success) (Houston and McNamara 1999). Alternative fitness measures include the geometric mean population growth and invasion fitness, which would increase the influence of poor years more than our current fitness measure. These fitness measures have advantages particularly if there is frequency dependence, bet hedging, or environmental fluctuations (Metz et al. 1992; Mylius and Diekmann 1995). Using these fitness measures would require changing to a modeling methodology where individual state is less resolved, for example, to the adaptive dynamics framework (Metz et al. 1992) or individual-based model with evolving traits, where explicit population dynamics makes fitness emergent (e.g., Strand et al. 2002).

Acknowledgements

Øyvind Fiksen from the University of Bergen and Ben Galuardi of the Large Pelagics Research Center from the University of Massachusetts Amherst provided critical insight and guidance to the development and writing of this work. The Bergen Research Foundation is thanked for funding of a research visit of EWC to the University of Bergen. This work was partially supported by NOAA grant NA04NMF455091 to M. Lutcavage and the Research Council of Norway (C. Jørgensen).

References

Block, B.A., Dewar, H., Blackwell, S.B., Williams, T.D., Prince, E.D., Farwell, C.J., Boustany, A., Teo, S.L.H., Seitz, A., Walli, A., and Fudge, D. 2001. Migratory movements, depth preferences, and thermal biology of Atlantic bluefin tuna. Science, **293**(5533): 1310–1314. doi:10.1126/science.1061197. PMID:11509729.

Block, B.A., Teo, S.L., Walli, A., Boustany, A., Stokesbury, M.J.W., Farwell, C., Weng, K., Dewar, H., and Williams, T.D. 2005. Electronic tagging and population structure of Atlantic bluefin tuna. Nature, **434**: 1121–1127. doi:10.1038/nature03463.

Brown, J.H., Gillooly, J.F., Allen, A.P., Savage, V.M., and West, G.B. 2004. Toward a metabolic theory of ecology. Ecology, **85**(7): 1771–1789. doi:10.1890/03-9000.

Carey, F.G., and Lawson, K.D. 1973. Temperature regulation in free-swimming bluefin tuna. Comp. Biochem. Physiol. A, **44**(2): 375–392. doi:10.1016/0300-9629(73)90490-8. PMID:4145757.

Clark, C.W., and Mangel, M. 2000. Dynamic state variable models in ecology. Oxford University Press, New York.

Corriero, A., Karakulak, S., Santamaria, N., Deflorio, M., Spedicato, D., Addis, P., Desantis, S., Cirillo, F., Fenech-Farrugia, A., Vassallo-Agius, R., Serna, J.M., Oray, Y., Cau, A., Megalofonou, P., and Metrio, G. 2005. Size and age at sexual maturity of female bluefin tuna (*Thunnus thynnus* L. 1758) from the Mediterranean Sea. J. Appl. Ichthyol. **21**(6): 483–486. doi:10.1111/j.1439-0426.2005.00700.x.

Cort, J.L. 1991. Age and growth of the bluefin tuna, *Thunnun thynnus* (L.) of the northeast Atlantic. Collect. Vol. Sci. Pap. ICCAT, **35**: 213–230.

DeAngelis, D.L., and Mooij, W.M. 2003. In praise of mechanistically-rich models. *In* Models in ecosystem science. *Edited by* C.D. Canham, J.J. Cole, and W.K. Lauenroth. Princeton University Press, Princeton, N.J. pp. 63–82.

Dunlop, E.S., Baskett, M.L., Heino, M., and Dieckmann, U. 2009. Propensity of marine reserves to reduce the evolutionary effects of fishing in a migratory species. Evol. Appl. **2**(3): 371–393. doi:10.1111/j.1752-4571.2009.00089.x.

Estrada, J.L., Lutcavage, M., and Thorrold, S.R. 2005. Diet and trophic position of Atlantic bluefin tuna (*Thunnus thynnus*) inferred from stable carbon and nitrogen isotope analysis. Mar. Biol. **147**(1): 37–45. doi:10.1007/s00227-004-1541-1.

Fish and Wildlife Service. 2009. Interior notice. Fed. Regist. **74**: 33 460–33 464.

Fitzgibbon, Q.P., Baudinette, R.V., Musgrove, R.J., and Seymour, R.S. 2008. Routine metabolic rate of southern bluefin tuna (*Thunnus maccoyii*). Comp. Biochem. Physiol. Part A: Mol. Integr. Physiol. **150**(2): 231–238. doi:10.1016/j.cbpa.2006.08.046.

Fromentin, J., and Powers, J.E. 2005. Atlantic bluefin tuna: population dynamics, ecology, fisheries and management. Fish Fish. **6**: 281–306.

Furnestin, J., and Dardignac, J. 1961. Le thon rouge de Maroc Atlantic (*Thunnus thynnus*). Rev. Trav. Inst. Pêch. Marit. **26**: 381–398.

Galuardi, B., Royer, F., Golet, W., Logan, J., Nielson, J., and Lutcavage, M. 2010. Complex migration routes of Atlantic bluefin tuna (*Thunnus thynnus*) question current population structure paradigm. Can. J. Fish. Aquat. Sci. **67**: 966–976. doi:10.1139/F10-033.

Garcia, A., Alemany, F., Velez-Belchi, P., Lopez Jurado, J., Cortes, D., de la Serna, J., Gonzalez Pola, C., Rodriguez, J., Jansa, J., and Ramirez, T. 2005. Characterization of the bluefin tuna spawning habitat off the Balearic Archipelago in relation to key hydrographic features and associated environmental conditions. Collect. Vol. Sci. Pap. ICCAT, **58**: 535–549.

Gleiss, A.C., Gruber, S.H., and Wilson, R.P. 2009. Multi-channel data-logging: towards determination of behaviour and metabolic rate in free-swimming sharks. *In* Tagging and tracking of marine animals with electronic devices. Series reviews: methods and technologies in fish biology and fisheries (REME), Vol. 9. *Edited by* J.L. Nielsen, H. Arrizabalaga, A. Hobday, and M. Lutcavage. Springer, the Netherlands. pp. 211–228.

Goldstein, J., Heppell, S., Cooper, A., Brault, S., and Lutcavage, M. 2007. Reproductive status and body condition of Atlantic bluefin tuna in the Gulf of Maine, 2000–2002. Mar. Biol. **151**(6): 2063–2075. doi:10.1007/s00227-007-0638-8.

Heinisch, G., Corriero, A., Medina, A., Abascal, F.J., de la Serna, J., Vassallo-Agius, R., Belmonte Rios, A., Garcia, A., de la Gandara, F., Fauvel, C., Bridges, C.R., Mylonas, C.C., Karakulak, S.F., Oray, I., de Metrio, G., Rosenfeld, H., and Gordin, H. 2008. Spatial-temporal pattern of bluefin tuna (*Thunnus thynnus* L. 1758) gonad maturation across the Mediterranean Sea. Mar. Biol. **154**(4): 623–630. doi:10.1007/s00227-008-0955-6.

Hewett, S.W., and Johnson, B.L. 1992. Fish bioenergetics model 2. University of Wisconsin, Sea Grant Institute, Madison, Wis.

Holdway, D.A., and Beamish, F.W.H. 1984. Specific growth rate and proximate body composition of Atlantic cod (*Gadus morhua* L). J. Exp. Mar. Biol. Ecol. **81**(2): 147–170. doi:10.1016/0022-0981(84)90003-0.

Houston, A.I., and McNamara, J.M. 1999. Models of adaptive behaviour: an approach based on state. Cambridge University Press, Cambridge, UK.

Inagake, D., Yamada, H., Segawa, K., Okazaki, M., Nitta, A., and Itoh, T. 2001. Migration of young bluefin tuna, *Thunnus orientalis* (Temminck et Schlegel), through archival tagging experiments and its relation with oceanographic condition in the Western North Pacific. Bull. Nat. Res. Inst. Far Seas Fish. **38**: 53–81.

ICCAT. 2007. Report of the 2006 Atlantic bluefin tuna stock assessment session (Madrid, Spain — June 12 to 18, 2006). Collect. Vol. Sci. Pap. ICCAT, **60**: 652–680.

ICCAT. 2009. Report of the 2008 Atlantic bluefin tuna stock assessment session (Madrid, Spain — June 23 to July 4, 2008). Collect. Vol. Sci. Pap. ICCAT, **64**: 1–352.

Itoh, T. 2006. Sizes of adult bluefin tuna *Thunnus orientalis* in different areas of the western Pacific Ocean. Fish. Sci. **72**(1): 53–62. doi:10.1111/j.1444-2906.2006.01116.x.

Jørgensen, C., and Fiksen, Ø. 2006. State-dependent energy allocation in cod (*Gadus morhua*). Can. J. Fish. Aquat. Sci. **63**(1): 186–199. doi:10.1139/f05-209.

Jørgensen, C., Ernande, B., Fiksen, Ø., and Dieckmann, U. 2006. The logic of skipped spawning in fish. Can. J. Fish. Aquat. Sci. **63**(1): 200–211. doi:10.1139/f05-210.

Jørgensen, C., Dunlop, E.S., Opdal, A.F., and Fiksen, Ø. 2008. The evolution of spawning migrations: state dependence and fishing-induced changes. Ecology, **89**(12): 3436–3448. doi:10.1890/07-1469.1. PMID:19137949.

Kitagawa, T., Kimura, S., Nakata, H., Yamada, H., Nitta, A., Sasai, Y., and Sasaki, H. 2009. Immature Pacific bluefin tuna, *Thunnus orientalis*, utilizes cold waters in the Subarctic Frontal Zone for trans-Pacific migration. Environ. Biol. Fishes, **84**(2): 193–196. doi:10.1007/s10641-008-9409-8.

Kooijman, S.A.L.M. 2000. Dynamic energy and mass budgets in biological systems. Cambridge University Press, UK.

Law, R., and Grey, D. 1989. Evolution of yields from populations with age-specific cropping. Evol. Ecol. **3**(4): 343–359. doi:10.1007/BF02285264.

Lawson, G.L., Castleton, M.R., and Block, B.A. 2010. Movements and diving behavior of Atlantic bluefin tuna *Thunnus thynnus* in relation to water column structure in the northwestern Atlantic. Mar. Ecol. Prog. Ser. **400**: 245–265. doi:10.3354/meps08394.

Lehodey, P., Senina, I., and Mortugudde, R. 2008. A spatial ecosystem and population dynamics model (SEAPODYM) — modeling of tuna and tuna-like populations. Prog. Oceanogr. **78**(4): 304–318. doi:10.1016/j.pocean.2008.06.004.

Logan, J. 2010. Tracking diet and movement of Atlantic bluefin tuna (*Thunnus thynnus*) using carbon and nitrogen stable isotopes. Ph.D. thesis, University of New Hampshire, Durham, N.H.

Lutcavage, M.E., Brill, R.W., Skomal, G.B., Chase, B.C., and Howey, P.W. 1999. Results of pop-up satellite tagging of spawning size class fish in the Gulf of Maine: Do North Atlantic bluefin tuna spawn in the mid-Atlantic? Can. J. Fish. Aquat. Sci. **56**(2): 173–177. doi:10.1139/f99-016.

Mather, F.J., and Shuck, H.A. 1960. Growth of bluefin tuna of the western North Atlantic. Fish Bull. **179**: 39–52.

Mather, F.J., Mason, J.M., and Jones, A.C. 1995. Historical document: life history and fisheries of Atlantic bluefin tuna. NOAA Tech. Memo. NMFS-SEFSC-370.

Medina, A., Abascal, F.J., Megina, C., and García, A. 2002. Stereological assessment of the reproductive status of female Atlantic northern bluefin tuna during migration to the Mediterranean spawning grounds through the Strait of Gibraltar. J. Fish Biol. **60**(1): 203–217. doi:10.1111/j.1095-8649.2002.tb02398.x.

Metz, J.A.J., Nisbet, R.M., and Geritz, S.A.H. 1992. How should we define fitness for general ecological scenarios? Trends Ecol. Evol. **7**(6): 198–202. doi:10.1016/0169-5347(92)90073-K. PMID:21236007.

Mylius, S.D., and Diekmann, O. 1995. On evolutionarily stable life histories, optimization and the need to be specific about density dependence. Oikos, **74**(2): 218–224. doi:10.2307/3545651.

Neilson, J.D., and Campana, S.E. 2008. A validated description of age and growth of western Atlantic bluefin tuna (*Thunnus thynnus*). Can. J. Fish. Aquat. Sci. **65**(8): 1523–1527. doi:10.1139/F08-127.

Overholtz, W.J. 2006. Estimates of consumption of Atlantic herring (*Clupea harengus*) by bluefin tuna (*Thunnus thynnus*) during 1970–2002: an approach incorporating uncertainty. J. Northwest Atl. Fish. Sci. **36**: 55–63. doi:10.2960/J.v36.m572.

Restrepo, V.R., Diaz, G.A., Walter, J.F., Neilson, S.E., Campana, S.E., Secor, D., and Wingate, R.L. 2010. Updated estimate of the growth curve of western Atlantic bluefin tuna. Aquat. Living Resour. **23**(4): 335–342. doi:10.1051/alr/2011004.

Rideout, G.A., Rose, G.A., and Burton, M.P.M. 2005. Skipped spawning in female iteroparous fishes. Fish Fish. **6**: 50–72.

Roff, D.A. 1983. An allocation model of growth and reproduction in fish. Can. J. Fish. Aquat. Sci. **40**(9): 1395–1404. doi:10.1139/f83-161.

Rooker, J.R., Bremer, J.R.A., Block, B.A., Dewar, H., de la Metrio, G., Corriero, A., Kraus, R.T., Prince, E.D., Rodriguez-Marin, E., and Secor, D.H. 2007. Life history and stock structure of Atlantic bluefin tuna (*Thunnus thynnus*). Rev. Fish. Sci. **15**(4): 265–310. doi:10.1080/10641260701484135.

Rooker, J.R., Secor, D.H., de Metrio, G., Schloesser, R., Block, B.A., and Neilson, J.D. 2008. Natal homing and connectivity in Atlantic bluefin tuna populations. Science, **322**(5902): 742–744. doi:10.1126/science.1161473. PMID:18832611.

Secor, D.H. 2002. Is Atlantic bluefin tuna a metapopulation? Collect. Vol. Sci. Pap. ICCAT, **54**: 390–399.

Secor, D.H. 2007. Do some Atlantic bluefin tuna skip spawning? Collect. Vol. Sci. Pap. ICCAT, **60**: 1141–1153.

Sibert, J.R., Lutcavage, M.E., Nielsen, A., Brill, R.W., and Wilson, S.G. 2006. Interannual variation in large-scale movement of Atlantic bluefin tuna (*Thunnus thynnus*) determined from pop-up satellite archival tags. Can. J. Fish. Aquat. Sci. **63**(10): 2154–2166. doi:10.1139/f06-114.

Strand, E., Huse, G., and Giske, J. 2002. Artificial evolution of life history and behavior. Am. Nat. **159**(6): 624–644. doi:10.1086/339997. PMID:18707386.

Teo, S., Boustany, A., and Block, B. 2007*a*. Oceanographic preferences of Atlantic bluefin tuna, *Thunnus thynnus*, on their Gulf of Mexico breeding grounds. Mar. Biol. **152**(5): 1105–1119. doi:10.1007/s00227-007-0758-1.

Teo, S.L.H., Boustany, A., Dewar, H., Stokesbury, M.J.W., Weng, K.C., Beemer, S., Seitz, A.C., Farwell, C.J., Prince, E.D., and Block, B.A. 2007*b*. Annual migrations, diving behavior, and thermal biology of Atlantic bluefin tuna, *Thunnus thynnus*, on their Gulf of Mexico breeding grounds. Mar. Biol. **151**(1): 1–18. doi:10.1007/s00227-006-0447-5.

Tiews, K. 1963. Synopsis of biological data on bluefin tuna *Thunnus thynnus* (Linnaeus) 1758 (Atlantic and Mediterranean). FAO Fish. Rep. Synopsis, **2**: 422–481.

Turner, S.C., and Restrepo, V.R. 1994. A review of the growth rate of West Atlantic bluefin tuna *Thunnus thynnus*, estimated from marked and recaptured fish. Collect. Vol. Sci. Pap. ICCAT, **42**: 170–172.

Turner, S., Restrepo, V.R., and Elkund, A. 1991. A review of the growth of Atlantic bluefin tuna, *Thunnus thynnus*. Collect. Vol. Sci. Pap. ICCAT, **35**: 271–293.

Varpe, Ø., Jørgensen, C., Tarling, G.A., and Fiksen, Ø. 2007. Early is better: seasonal egg fitness and timing of reproduction in a zooplankton life-history model. Oikos, **116**(8): 1331–1342. doi:10.1111/j.0030-1299.2007.15893.x.

Vogel, S. 1994. Life in moving fluids: the physical biology of flow. Princeton University Press, Princeton, N.J.

Walli, A., Teo, S.L.H., Boustany, A., Farwell, C.J., Williams, T., Dewar, H., Prince, E., and Block, B.A. 2009. Seasonal movements, aggregations and diving behavior of Atlantic bluefin tuna (*Thunnus thynnus*) revealed with archival tags. PLoS ONE, **4**(7): e6151. doi:10.1371/journal.pone.0006151. PMID:19582150.

Ware, D.M. 1978. Bioenergetics of pelagic fish: theoretical change in swimming speed and ration with body size. J. Fish. Res. Board Can. **35**(2): 220–228. doi:10.1139/f78-036.

White, C.R., Phillips, N.F., and Seymour, R.S. 2006. The scaling and temperature dependence of vertebrate metabolism. Biol. Lett. **2**(1): 125–127. doi:10.1098/rsbl.2005.0378. PMID:17148344.

Wieser, W. 1994. Cost of growth in cells and organisms: general rules and comparative aspects. Biol. Rev. Camb. Philos. Soc. **69**(1): 1–33. PMID:8193215.

Wilson, S.G., Lutcavage, M.E., Brill, R.W., Genovese, M.P., Cooper, A.B., and Everly, A.W. 2005. Movements of bluefin tuna (*Thunnus thynnus*) in the northwestern Atlantic Ocean recorded by pop-up satellite archival tags. Mar. Biol. **146**(2): 409–423. doi:10.1007/s00227-004-1445-0.

Appendix A

Figure A1 appears on the following page.

Fig. A1. Results from secondary sensitivity analyses. The mean length-at-age from model output when each parameter in Table 3 is varied above (solid line) and below (dot-dashed line) its baseline value (dotted line). The age at 50% maturity for each simulation is indicated by a black square.